Environmental Science & Technology

Article

pubs.acs.org/est

Continuous Flow Analysis of Labile Iron in Ice-Cores

William T. Hiscock,* Hubertus Fischer, Matthias Bigler, Gideon Gfeller, Daiana Leuenberger, and Olivia Mini

Climate and Environmental Physics, Physics Institute, University of Bern, Sidlerstrasse 5, CH-3012 Bern, Switzerland

Supporting Information

ABSTRACT: The important active and passive role of mineral dust aerosol in the climate and the global carbon cycle over the last glacial/interglacial cycles has been recognized. However, little data on the most important aeolian dust-derived biological micronutrient, iron (Fe), has so far been available from ice-cores from Greenland or Antarctica. Furthermore, Fe deposition reconstructions derived from the palaeoproxies particulate dust and calcium differ significantly from the Fe flux data available. The ability to measure high temporal resolution Fe data in polar ice-cores is crucial for the study of the timing and magnitude of relationships between geochemical events and biological responses in the open ocean. This work adapts an existing flow injection analysis (FIA) methodology for low-level trace Fe determinations with an existing glaciochemical analysis system, continuous flow analysis (CFA) of ice-cores. Fe-induced oxidation of *N,N′*-dimethyl-*p*-pheylenediamine (DPD) is used to quantify the biologically more important and easily leachable Fe fraction released in a controlled digestion step at pH ∼1.0. The developed method was successfully applied to the determination of labile Fe in ice-core samples collected from the Antarctic Byrd ice-core and the Greenland Ice-Core Project (GRIP) ice-core.

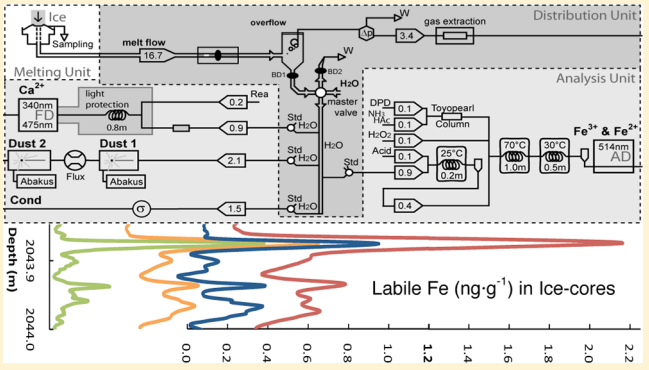

INTRODUCTION

Glaciochemical data from ice-core records represent key information on past long-term atmospheric changes but also on interannual to decadal atmospheric variability, seasonal variations, and past abrupt climate change. For example, time series for major ion (e.g., Na^+, Ca^{2+}, and Mg^{2+}) concentrations reveal dramatic and abrupt changes in sea salt and mineral dust aerosol production during glacial and interglacial periods[1−3] and provided insight into their forcing mechanisms.[4] On the other hand, analyses of air bubbles trapped in Antarctic ice-cores reveal that atmospheric CO_2 increased by up to 20 ppmv during Antarctic warm events,[5,6] and atmospheric CO_2 concentrations are generally anticorrelated to dust flux and temperature in Antarctica.[7]

At global scales, dust is a major source of minerals[8] and associated nutrients[9] to the ocean. Dissolved Fe concentrations are believed to play a key role in controlling biological productivity[10] despite the abundance of major nutrients in high-nutrient low-chlorophyll (HNLC) regions such as the Southern Ocean.[11] Iron limitation in the remote ocean may influence many phytoplankton physiological processes: including photosynthetic energy conversion efficiency,[12] nitrate assimilation,[13] chlorophyll synthesis,[14] and elemental stoichiometry.[15] Therefore, the change in aerosol-derived Fe flux to the ocean during glacial/interglacial transitions is believed to play a relevant role in controlling oceanic phytoplankton uptake of atmospheric CO_2. Accordingly, high quality Fe records from ice-cores can shed light on the influence of dust fertilization on atmospheric CO_2 changes.[16] In this respect, the seasonal phasing of biological productivity, sea ice coverage, and Fe input by aeolian mineral dust aerosol may become crucial, requiring seasonally resolved Fe records from ice-cores over glacial/interglacial time scales.

The Division for Climate and Environmental Physics (CEP) at the Physics Institute, University of Bern, has developed a unique CFA system for the spectrometric analysis of ionic tracers and for specific gas tracers on ice-cores.[17−20] Records have added substantially to our understanding of changes in past atmospheric circulation, the climate conditions in aerosol source areas,[3,21] and the change in biogeochemical cycles[22] over the last 800 000 years. The Bern-CFA method provides contamination-free meltwater and allows for very high (often seasonal) resolution. In contrast, sample preparation of discrete sampling techniques for leachable trace elements[23] utilize lengthy digestion procedures (>24 h), have relatively coarse depth resolution, and introduce sample handling and sample bottle storage artifacts. In addition, CFA inductively coupled plasma mass spectrometry (ICP-MS) techniques[24] and discrete sample procedures do not separate insoluble and soluble fractions before ICP-MS analysis. Elemental analyses of the combined insoluble and soluble fractions made with ICP-MS

Received: November 17, 2012
Revised: March 24, 2013
Accepted: April 1, 2013
Published: April 1, 2013

are method dependent, with particles as large as 0.1 μm being vaporized before the ions produced from the particle are sampled by the mass spectrometer.[25,26]

The ability to measure biologically important trace elements with high temporal resolution will allow for investigation of high-frequency phenomena observed in the ice-core record (i.e., seasonal cycles and year-to-year variation) and rapid climate change events such as those during the Holocene–Younger Dryas transition, when Greenland ice-core records suggest that major changes in climate occurred over a few decades or less.[27] Thus, assessing the Fe fraction available for biological productivity or the easily leachable labile fraction of aeolian metal depositions in ice-cores is essential to constrain the carbon cycle/climate feedback and provide data necessary to improve our understanding of biogeochemical processes in the palaeocean and to model past and future changes.

Accordingly, in this study we concentrated on the methodological aspects to quantify the labile fraction of Fe in a sensitive, continuous, and field-deployable CFA setup using the Fe-induced oxidation of *N*,*N*′-dimethyl-*p*-phenylenediamine (DPD). In our approach, the CFA methodology for sample treatment and digestion in a dilute acid over a discrete period of time operationally defines the leachable fraction of Fe and represents our methodological definition of the labile fraction of Fe. This easily leachable fraction at pH ∼1.0 (0.024 M Q-HCl) represents all but the most refractory metal species released into dissolved form (Fe_D). A similar approach by Spolaor et al.[28] based on previous work by Traversi et al.[29] was developed contemporaneously with our investigation. In our study we made significant improvements in the detection chemistry that allow for stable and high precision Fe detection in a completely field-deployable setup. Here we present our new Fe analytical method in detail, providing a rigorous quantification of the figures of merit of this method, and explain the improvements made compared to previous attempts. We test our method on selected ice-core segments from Greenland and Antarctica; however, a more systematic study of the pH dependence of Fe release in our online digestion method and the issue of which Fe fraction is best reflecting bioavailable iron in aeolian dust fertilization is beyond the scope of this paper and will be tackled in future studies.

METHOD

The analytical method for measuring Fe is based on a spectrophotometric determination and takes advantage of the ability of the Fe^{3+} ion to oxidize the *N*,*N*′-dimethyl-*p*-phenylenediamine (DPD) to the semiquionic form (DPDQ) in the presence of hydrogen peroxide (H_2O_2). Determinations of DPDQ concentration are quantified by spectrophotometer absorbance measurements at a wavelength of 514 nm and yield a signal proportional to the amount of the sum of both dissolved Fe^{2+} and Fe^{3+} species present in the sample. Surface dissolution of Fe from dust particles suspended in ice-core meltwater is developed in the reaction coil, and dissolved iron concentrations, [Fe_D], are determined in the analytical module.

The protocols using the CFA sampling system, the analytical techniques for measuring Fe_D, and the cleaning procedures are comparable with other currently accepted sampling methodologies, analytical techniques, and protocols utilized during the NSF-sponsored Sampling and Analysis of Iron (SAFe) intercomparison cruise.[30,31] All solutions were prepared in acid-cleaned low-density polyethylene (LDPE) plastic ware with ultrahigh purity water (UHP-H_2O) of resistivity >18 MΩ·cm. All sample handling and reagent preparation were carried out in a Class-100 environment using trace metal clean techniques. Details for the reagents [trace metal grade hydrochloric acid (Q-HCl); Fe Standards; ammonium acetate (NH_3/HAc) solution; hydrogen peroxide (H_2O_2); and *N*,*N*′-dimethyl-*p*-phenylenediamine (DPD) in a sodium sulfite (Na_2SO_3) solution with triethylenetetramine (TETA) and later referred to as preserved DPD (pDPD)] are provided in the Supporting Information.

Bern-CFA. The Bern-CFA system is able to resolve transient climate signals in ice-core layers of ∼1 cm thickness for insoluble particles and their size distribution (dust), Na^+, Ca^{2+}, NH_4^+, NO_3^-, SO_4^{2-}, H_2O_2, HCHO, and specific electrolytic conductivity (σ). The Bern-CFA system consists primarily of a melting unit in a freezer, a debubbler, sample/standard valves, and various analytical modules in a lab at normal room temperature (∼+20 °C). Details and a schematic (Figure S1) of the Bern-CFA system are provided in the Supporting Information and have been previously described in detail.[32,33]

Labile Fe Detection. To evaluate the bioavailability and environmental mobility of aeolian Fe deposition archived in ice-cores, the easily leachable fraction is analyzed; ice-core samples are digested for leachable Fe and determined for the dissolved Fe (Fe_D). The CFA methodology sample treatment and digestion operationally define what fraction of the total Fe (Fe_T) contained in the ice-core is being measured. Samples are acidified in-line with Q-HCl to form a final concentration of 0.024 M Q-HCl (pH ∼1.0). The digestion acid (0.1 mL·min^{-1}), sample (0.9 mL·min^{-1}), and air (0.1 mL·min^{-1}) are combined and maintained as a segmented flow in a 0.2 m reaction coil at +25 ± 0.1 °C for approximately 30 s (Figure S1). The chemical method of analysis distinguishes between the free and labile complexed forms of dissolved Fe species available for measurement from the undetectable refractory Fe contained within suspended particulate matter. The analyte and the definition for Fe_D in the study is therefore operationally defined as the free Fe species and labile complexed Fe species available and release from bound refractory Fe resulting from the sample pretreatment described above. Note that in principle the degree of digestion and Fe release could be varied by appropriate acid addition, temperature increase, and period of digestion prior to spectrometric quantification.

Precleaning of the DPD solution is a critical procedure, as DPD is documented to be contaminated with Fe.[34−36] The H_2O_2 reagent (0.1 mL·min^{-1}), acidified sample (0.4 mL·min^{-1}), and pH-adjusted DPD/NH_3/HAc mixture (0.2 mL·min^{-1}) are combined and flow through two reaction coils at elevated temperatures. Absorbance is measured over a 10 mm optical path length at 514 nm. Details of the labile Fe detection system are provided in the Supporting Information.

RESULTS

Sensitivity Optimization. The visible absorption spectrum for DPDQ presents two equal maxima at 514 and 552 nm. Determination of DPDQ concentrations at 514 nm yield a signal proportional to the [Fe_D] present in the digested water-suspended-solid sample of ice-core meltwater. The sensitivity and reproducibility of absorbance measurements are enhanced through the optimization of analytical parameters. Reaction temperature and stability contribute significantly to sensitivity and reproducibility of absorbance measurements. Increasing the reaction temperature in the primary reaction coil accelerates the catalyzed reaction rate of DPD. The reported reaction coil

temperatures represent the temperature set point for the heated primary reaction coil. Figure S2A (Supporting Information) shows increasing reaction coil temperature (°C) yields increasing sensitivity. The expanded uncertainty (3σ) for measurements is found to be high at lower temperatures, where depressed reaction rates lead to little color development, lower concentrations of DPDQ, and therefore increased variability. The expanded uncertainty for measurements is found to be also high at elevated reaction coil temperatures greater than +70 °C. Erratic reaction mixture behavior specifically results from the accelerated decomposition of H_2O_2, which occurs via complicated reaction mechanisms and dependent on several parameters (i.e., reaction media, temperature, pressure, contact surfaces, etc.). Maintaining the primary reaction coil temperature at +70 °C minimizes the decomposition of H_2O_2 and microbubble formation, while maintaining high sensitivity and low expanded uncertainty.

The effect of reaction mixture pH on the sensitivity and uncertainty of the reaction of DPD in the presence of the Fe^{3+} and H_2O_2 is depicted in Figure S2B. Investigations examine the pH range 4.0−7.0, with pH measured in the effluent after absorbance measurements and at +20 °C. The final reaction mixture pH results in variations in the reaction rate of DPD to the semiquionic form DPDQ and ultimately the sensitivity of the analytical method. The expanded uncertainty of the standards and sensitivity of the reaction shows a wide pH range (4.5−5.5) with similar sensitivity and uncertainty. The optimal reaction mixture pH is 5.1 ± 0.1 determined by analytical sensitivity ($\gamma = b_1/\sigma$, where b_1 is the absorption sensitivity in absorption units per nM Fe), which includes precision in sensitivity definition. Therefore, the optimal pH was found at the confluence of high sensitivity and low uncertainty. Results in Figure S2B are obtained with a 0.5 M NH_3/HAc solution, a reaction mixture concentration of 0.12 M H_2O_2, and 0.0015 M DPD. Results investigating the optimal pH are in agreement with the more recent results investigating Fe_D in water by FIA.[37]

The effect of the H_2O_2 concentration on the sensitivity and uncertainty of the reaction DPD in the presence of the analyte Fe is depicted in Figure S2C. The reaction sensitivity increases linearly with the $\log[H_2O_2]$, for reaction mixture concentration below 0.44 M H_2O_2. At reaction mixture concentrations above 0.44 M H_2O_2, there is an appreciable decrease in reaction sensitivity. The strong oxidizing power of H_2O_2 activated with the catalyst Fe can rapidly destroy easily oxidized organic compounds (i.e., DPD) with free radicals. Alternatively, the strong oxidizing power of H_2O_2 may also force the colored intermediate product from the long-lived resonance stabilized semiquinoid structures to the relatively unstable quinonoid structures and final colorless reaction product, similar to the oxidation intermediates and reaction products of *N,N′*-diethyl-*p*-phenylenediamine.[38] Whatever the mechanism, reaction mixture H_2O_2 concentrations above 0.44 M result in decreased reaction sensitivity. Results show that reaction mixture H_2O_2 concentrations above 0.15 M show increasing sensitivity; however, uncertainty in the measurement increased as the short reaction time and high absorbance produced a less stable signal. Optimal sensitivity in conjunction with lowest uncertainty occurs at a reaction mixture H_2O_2 concentration of 0.123 M for results obtained with a 0.2 M ammonium acetate solution and a reaction mixture concentration of 0.0030 M DPD.

The sensitivity and uncertainty of measurements for the determination of Fe_D for varying reaction mixture concentrations of DPD are investigated in a 0.5 M ammonium acetate solution and reaction mixture concentration of 0.25 M H_2O_2. Solutions of DPD are prepared by the addition of crystalline DPD to 500 mL of 2.0×10^{-3} M Na_2SO_3 solution. The effect of reaction mixture DPD concentration on the oxidation rate of DPD in the presence of the homogeneous catalysts Fe^{3+} and H_2O_2 is depicted in Figure S2D. The reaction sensitivity increases linearly with reaction mixture concentrations $<1.5 \times 10^{-3}$ M DPD. As the reaction is occurring in a closed system, the increased reaction rate is explained by collision theory. At reaction mixture concentrations above 1.5×10^{-3} M DPD, there is a clearly defined plateau in reaction sensitivity. The reactants in the closed system are consumed, resulting in the observed plateau in reaction sensitivity. The expanded uncertainty or 3σ for measurements is found to be higher at concentrations above 1.5×10^{-3} M DPD due to erratic behaviors caused by the accelerated decomposition of H_2O_2 and high absorbencies producing a less stable signal; optimal analytical sensitivity occurs at a reaction mixture concentration of 1.5×10^{-3} M DPD.

Novel DPD Reagent Chemistry. Maintaining DPD in a reduced (colorless) form before quantitative reaction with the analyte Fe is an important condition for reliable measurements with this method and limited its use in previous attempts.[36] Over the course of the analytical sequence, a decrease in sensitivity, a narrower linear dynamic range, and an increase in baseline is usually observed, as the uncatalyzed reaction persists in the DPD reagent solution. DPD in an acidic medium (aDPD) and Fe^{3+} as the dominant hydrolysis species minimize the reagent blank value by inhibiting the formation of DPDQ. Earlier methods have typically prepared a 0.050 M DPD solution in 0.002 M Q-HCl and pH ∼2.2,[36] fresh at the commencement of an 8 to 12 h analytical sequence. Nevertheless, color development and oxidation of DPD solutions occur and largely result from the uncatalyzed redox reaction, which proceeds at pH ∼2.2. The uncatalyzed redox reaction is pH dependent with an optimum range of pH 2−3.[39] Here sodium sulfite, Na_2SO_3, an oxygen scavenger agent, is used to protect DPD solutions from oxidation.

Long-term storage of solid DPD before reagent preparation is another weakness for shipboard analysis and fieldwork, a prerequisite that presents additional problems. The condition of stored DPD solid reagent used to prepare reagent solutions at the beginning of each analytical sequence significantly affects sensitivity, with the sensitivity of stored DPD solid reagent varying as much as 10% between different preparations for analytical sequences. The reducing environment of a Na_2SO_3 solution and the acidic medium preserves the DPD, with pDPD solutions of 0.020 M DPD in 2×10^{-4} M Na_2SO_3 stored in the dark at +4 °C in sealed LDPE bottles showing no observable color development and no measurable reduction in reaction sensitive after 280 days.

Although Na_2SO_3 as an oxygen scavenger agent protects a DPD solution from oxidation and maintains the prepared dissolved DPD reagent in a reduced form, commercially available DPD·2HCl is notoriously contaminated with divalent metals. The presence of Fe impurities in DPD results in the oxidation of DPD and the immediate color development upon pH adjustment and introduction of H_2O_2, which result in significant reagent blanks and elevated baselines despite preservation efforts. The reducing environment of a Na_2SO_3

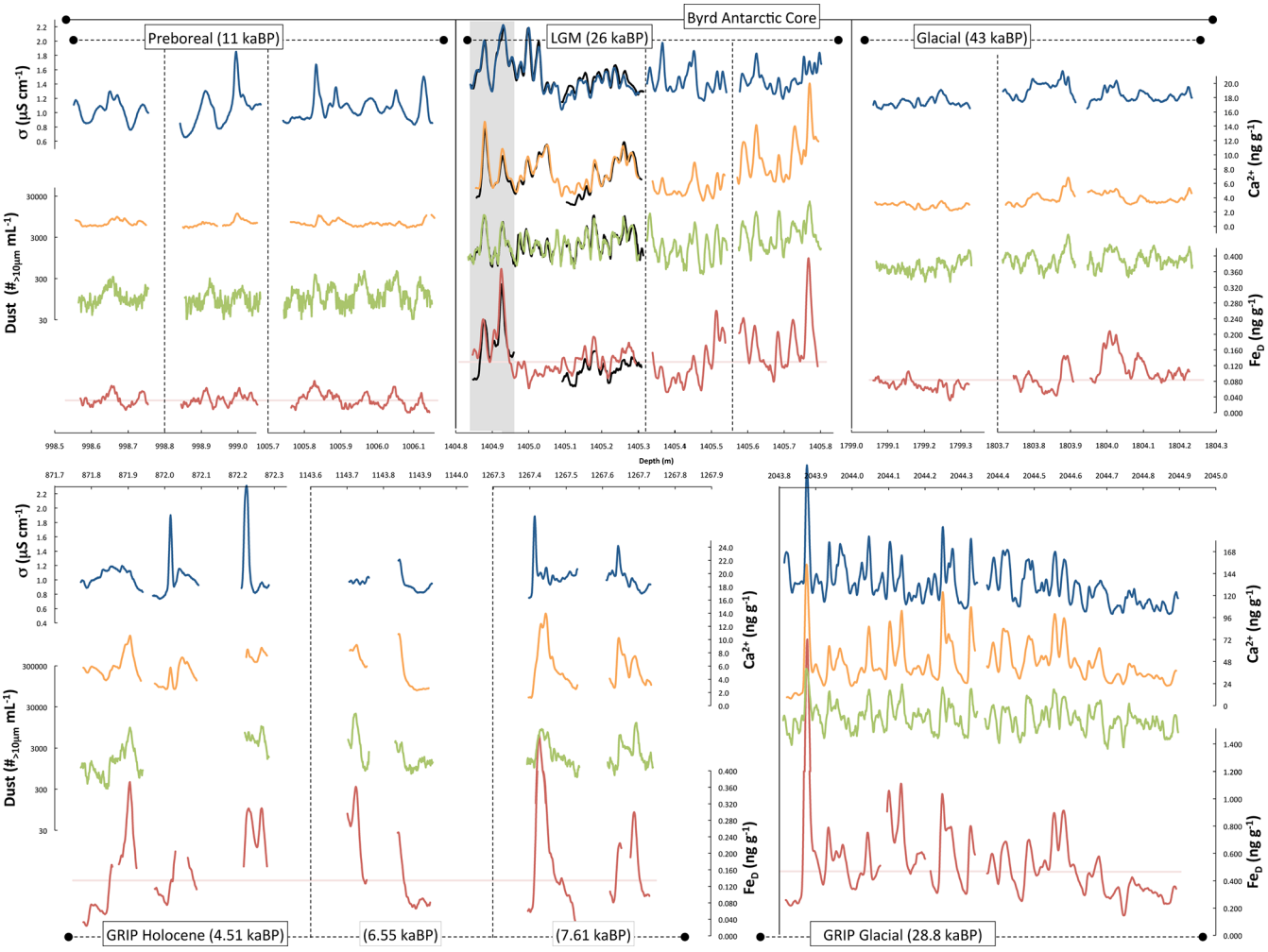

Figure 1. CFA measurements of conductivity (σ), Ca^{2+}, dust, and Fe_D determined on ice-core sections from the Antarctic Byrd ice-core (1968) and the GRIP ice-core (GRIP 1992): The solid horizontal line represents the median of 1 mm ice-core depth bin averages for Fe_D determined over the analyzed core length. The solid black lines represent replicate measurements. The gray area represents a region of an ice-core section, where not all particulate dust events and the corresponding conductivity and Ca^{2+} peaks vary equally with [Fe_D]. Conductivity (σ), blue. Ca^{2+}, orange. Dust, green. Fe_D, red.

solution enables the efficient immobilization of trace metal contaminates from the preserved DPD reagent (pDPD) solution with the Toyopearl-AF-Chelate-650 resin, minimizing the increase in the analytical baseline before catalytic reaction with H_2O_2. A concentration $\leq 3.0 \times 10^{-5}$ M Na_2SO_3 preserves the DPD from oxidation and is efficiently oxidized to sulfate (SO_4^{2-}) in the reaction solution by the strong oxidizing capacity of H_2O_2.

The Na_2SO_3 in the pDPD ultimately has no effect on the reaction sensitivity, as increasing the reaction mixture H_2O_2 concentration counterbalances any decrease in reaction sensitive resulting from the oxidation of sulfite (SO_3^{2-}) with H_2O_2. Furthermore, results indicate that a concentration $\leq 3.0 \times 10^{-5}$ M Na_2SO_3 in the reaction solution presents no interferences with the catalytic reaction or absorbance measurements. The resulting concentrations of SO_4^{2-} in the reaction mixture is significantly lower than the ~0.01 M SO_4^{2-} found in the reaction solutions of previous methods utilizing seawater (0.0282 M SO_4^{2-}, S = 35) as a carrier solution.[34−36] Results indicate that the sensitivity, uncertainty, and baseline maintain a tight range over a period of 100 days. The variation in sensitivity and uncertainty between different analytical sequences is dramatically reduced in comparison to the method utilizing aDPD (Figure S3, Supporting Information).

Method Validation. Quality assurance and quality control (QA/QC) of data and methods were validated by measurements prepared from the primary stock standard solution, a traceable certified reference material. Metal concentrations were quantified by calibrations against acidified working standards (0.002 M Q-HCl) prepared from a serial dilution of the secondary stock standard solution (50.05 ng·kg^{-1}, 1003.7 nM Fe in 0.024 M Q-HCl). A standard curve for calibrating the analytical chemical determinations for typical CFA analyses utilized four working standards (0, 0.056, 0.279, and 2.668 ng·g^{-1} Fe in 0.002 M Q-HCl). Blanks were prepared in the same manner as that for the sample to ensure experimental quality. Time series and calibration curves of an eight-point calibration are depicted in Figure S4, Supporting Information. A least-squares linear regression analysis provides a calibration curve and data for the limit of linearity, the limit of detection (LOD), sensitivity, and expanded uncertainty for the analytical method (Table S1, Supporting Information). The continuous meltwater technique of the Bern-CFA system is capable of chemical analysis at slow ice-core melting rates (1.5 to 4

dx.doi.org/10.1021/es3047087 | Environ. Sci. Technol. 2013, 47, 4416−4425

cm·min^{-1}), and results demonstrate high depth resolution for Fe analysis. The determinations of Fe_D equate to a depth resolution of 2.38 cm and are calculated from a Fe_D time resolution of 43 s ± 5% (Figure S4) and the ice-core melt speed of 3.34 ± 0.24 cm·min^{-1}. The temporal resolution value is an average calculated from the time difference as the signal changes from 10% to 90% signal height for the measurement of standards of different concentration. In comparison, the depth resolution of the electrolytic conductivity is 4× greater and the depth resolution of Ca^{2+} is 2× greater than the depth resolution for Fe analysis.

Baseline and standard measurements utilizing the CFA sample delivery system are comparable to measurements bypassing the CFA sample delivery system. Baseline measurements of synthetic ice-core samples prepared from degassed UHP-H_2O and sampled from the ice-core melthead are comparable to those from UHP-H_2O bypassing the ice-core melthead. Baseline measurements of Fe_D in synthetic ice-core samples yield a LOD = 0.028 ng·g^{-1} and 3σ = 0.033 ng·g^{-1}. The test measurements on synthetic ice-core samples demonstrate typical run behaviors in comparison with true ice-core samples; i.e., anomalous analysis peaks correlating with the start of an ice-core melt sequence, recorded breaks between ice-core samples, and the termination of an ice-core melt sequence.

Measurements of Fe_D were performed on real ice-core samples from the Antarctic Byrd ice-core and from the GRIP ice-core. Ice-core sections were prepared for CFA analysis in a −20 °C freezer. The first determinations of [Fe_D] using our new CFA method were performed on ice-core sections from the Antarctic Byrd ice-core for three time intervals: preboreal ice (∼11 kaBP), ice from the LGM (∼22.6 kaBP), and glacial ice (∼43 kaBP) (Figure 1). The Antarctic Byrd ice-core represents a low dust regime, and for the preboreal ice-core section, Fe_D concentrations are found in a narrow range (0.03−0.09 ng·g^{-1}) with the lower end of the measured concentration range just above the LOD. Even with the low particulate dust counts for this low dust regime, [Fe_D] show a close correspondence in depth variation with dust counts. [Fe_D] are found over a wider range (0.03−0.40 ng·g^{-1}) for ice-core sections from the LGM. Replicate measurements performed on duplicate ice-cores show remarkable agreement with an average offset 0.023 ± 0.024 ng·g^{-1} (Figure 1), which is less than the expanded uncertainty (3σ) of 0.05 ng·g^{-1}. Moreover, this offset could be corrected for by applying a drift correction to the baseline. Additionally, the measured [Fe_D] profiles from the LGM show that not all particulate dust events and the corresponding conductivity and Ca^{2+} peaks vary equally with [Fe_D] (Figure 1); nonuniformities are further revealed by Fe_D:dust and Ca^{2+}:dust ratios (Figure S5, Supporting Information). The nonuniformities suggest that [Fe_D] are independent of the magnitudes of individual dust events and justify the increased analytical effort for direct Fe quantification as presented in this study.

Further analyses of [Fe_D] are completed on Holocene ice (brittle zone) and glacial ice (∼28.8 kaBP) during a Dansgaard−Oeschger (D-O) event from the GRIP ice-core (Figure 1). The Greenland ice-cores represent a much higher dust regime compared to the Antarctic Byrd ice-core, with dust events 2 orders of magnitude greater than the measured Antarctic ice-core sections. [Fe_D] for GRIP Holocene are found in a narrow range (0.05−0.50 ng·g^{-1}), [Fe_D] for GRIP glacial ice during a D-O event are found over a wide range (0.20−2.40 ng·g^{-1}), and [Fe_D] are in close correspondence with the depth variations in σ, Ca^{2+} and particulate dust.

DISCUSSION

The developed method expands upon earlier work[28,29] with improved chemistry and simplification of the reaction manifold. Chemical parameters are optimized within the constraints of established operating protocol for system variables of the existing Bern-CFA methodology. Methodological constraints include a predetermined constant peristaltic pump speed of ∼300 cm·min^{-1}, a maximum sample introduction flow rate of 0.9 mL·min^{-1}, and a reaction manifold with a short transit time (<2 min.). Furthermore, the method was developed, assembled, and optimized by only utilizing existing, standardized, and interchangeable Bern-CFA components in the reaction manifold (i.e., primary heated reaction coil −1 m and a secondary cooled reaction coil −0.5 m).

The developed method provides precise determination of labile Fe present in ice-core samples at nanomolar levels (1.0 nM Fe = 0.056 ng·g^{-1}, 56 ppt) without the analytical requirement of preconcentration, greatly simplifying the reaction manifold and reducing the reagent requirements. Compared to previous work,[28,29] our method includes precleaning of the DPD reagent. The presence of Fe impurities in DPD results in the oxidation of DPD and immediate color development, which would result in significantly higher reagent blanks and elevated baselines. Moreover, our chemically stabilized DPD reagent allows for much improved long-term measurement stability and makes the time-consuming preparation of fresh DPD reagent unnecessary. This becomes a crucial issue for the long-term field deployability of this method. Removal of the sample preconcentration step in the FIA method[34,35] eliminates the requirement for strong eluting acid and demands a smaller buffering capacity for NH_3/HAc solution. The developed CFA method for Fe relies on improved temperature stabilization throughout the manifold. A series of temperature-regulated mixing coils enhance the reaction rate and generate a reproducible reaction rate. An accurate adaptation of FIA methods,[34,35] improved temperature stabilization, and the implementation of standardized, well-known trace element protocols also improve our method.

A chelating resin derivatized with iminodiacetic acid (Toyopearl-AF-Chelate-650) is used to immobilize metals for the extraction and precleaning of DPD. The primary reason for utilizing Toyopearl resin is the commercial availability, thus yielding consistent and reproducible results for the efficiency of extraction and recovery of trace elements as compared to 8-HQ chelating resin. Second is the widely accepted utilization of this resin for the analysis of trace elements, i.e., Toyopearl-AF-Chelate-650 resin is employed to process seawater for the preconcentration trace element and matrix elimination in flow injection ICP-MS analysis[40] and isotope dilution ICP-MS analysis.[41] The Toyopearl resin displays high extraction efficiency at room temperatures (∼20 °C) and small resin volumes (700 μL), which result in less back-pressure and baseline modulation. Adsorption of Fe on Toyopearl-AF-Chelate-650 resin is highest at the pH range of 6.1−6.5 and in agreement with the reported optimal Fe extraction pH 6.4 ± 0.1.[42] The mildly reducing environment of the 2 × 10^{-4} M Na_2SO_3 DPD solution and the optimized resin extraction pH 6.2 results in a lower reaction rate and lower concentration DPDQ during the in-line precleaning procedure of the DPD

dx.doi.org/10.1021/es3047087 | Environ. Sci. Technol. 2013, 47, 4416−4425

reagent, ultimately resulting in a lower, more stable baseline for the analytical method and for the determination of Fe.

The reaction chemistry is optimized for the water-suspended solid matrix of ice-core meltwater as compared to the low Fe seawater matrix of the FIA method. Optimization for a pure H_2O matrix and removal of the preconcentration step altered the requirements of the reaction mixture concentration for most reagents, specifically the reagent TETA. Results show that a reaction mixture concentration of TETA typical of FIA methods with a seawater matrix decreased the sensitivity of Fe_D determinations in the CFA method, where Fe is contained in a pure H_2O matrix with lower contaminate divalent metal ion concentrations. The optimized concentration of 4.0×10^{-7} M TETA in the reaction mixture preserves the sensitivity and detection limit of the method. Second, investigations scrutinizing the optimal pH of the reaction mechanism for the catalytic oxidation of DPD in the presence of Fe^{3+} and H_2O_2 are inconsistent with earlier FIA methods. The optimal reaction mixture pH is 5.1 ± 0.1, significantly lower and outside the reported range (pH 5.5−6.0) of earlier results.[35]

Preservation of DPD allows for the preparation, standardization, and long-term storage of DPD reagent. The introduction of the oxygen scavenging agent/reducing agent Na_2SO_3 to the DPD reagent preserves DPD in a reduced colorless form. Solutions of 0.010 M DPD in 1×10^{-4} M Na_2SO_3 stored in the dark at room temperature in sealed LDPE bottles show no observable color development and no measurable reduction in reaction sensitive after 280 days. Therefore, the variation in sensitivity and uncertainty of the data set are dramatically reduced for a series of analytical sequences and the ability to quality control the data set, discern contributions of systematic error, and assist in the diagnosis of problems is improved. The addition of Na_2SO_3 to the DPD reagent is also directly applicable to the current FIA method used in the field for seawater analysis,[35] halting the uncatalyzed redox reaction and successfully preserving DPD solutions for the duration of an 8−12 h analytical sequence. Furthermore, the preservation of the DPD reagent provides the potential for the offline precleaning of the DPD reagent, while advancing the possibility of automated Fe determinations and its suitability for long-term remote deployment. We also investigated the offline precleaning of contaminate trace elements in DPD by coprecipitation, providing a DPD reagent that is not only stable but further simplifies existing FIA.[35] Preliminary results are promising, and the method utilizing a DPD oxalate represents a possible breakthrough for autonomous and long-term measurement campaigns. The bulk precipitate, calcium oxalate, coprecipitates contaminate trace elements and produces a stable DPD reagent with low Fe reagent blank from the commercially available DPD oxalate. Additional studies could build on the initial exploratory work by investigating high purity calcium sulfite as primer for the calcium oxalate bulk precipitate in a DPD oxalate solution and by investigating increasing time of contact of the DPD solution with the bulk precipitate. However, the online precleaning of the DPD solution using the Toyopearl chelating resin provided sufficient results within the time frame of this study. While there is a need within palaeogeochemistry to be able to obtain data sets for the biogeochemically active fraction of trace elements in ice-cores, the novel chemistry utilized for the preservation of the DPD reagent introduces the possibility of adapting the spectrophotometric method for use on long-term autonomous buoys and the ability to monitoring pelagic, littoral, and estuarine environments.

Results demonstrate the successful adaptation of a colorimetric method for the determination of Fe_D operating in parallel with existing methodologies used by the Bern-CFA system for ice-cores. The continuous meltwater technique of the Bern-CFA system is demonstrated to have the advantage to avoid contamination of samples for trace Fe analysis and, with its improved figures of merit (see Table S1), allows for reliable continuous analyses of trace levels in polar ice-cores. The LOD (0.031 $ng \cdot g^{-1}$) is 40% lower but still in the same range as the one given by Spolaor et al.[28] However, we expect a significant improvement in continuous long-term stability of the results due to our improved reagent chemistry. Our method also features an extended limit of linearity ranging up to 4 $ng \cdot g^{-1}$and allows for reliable quantification of the dynamic Fe signal of Greenland ice-cores during glacial periods.

Validation of the method is supported by the coregistration of CFA measured analytes and shown by the close correspondence in depth variation of conductivity (σ), Ca^{2+} and dust on archived ice-core sections from the Antarctic Byrd ice-core (1968) and GRIP ice-core (1992). No correlation between ice-core breaks and chemical measurements are found, suggesting that existing ice-core handling and cutting procedures at the University of Bern are also sufficient for trace metal analysis. Further validation is provided by the reproducibility in analyses on duplicate ice-cores prepared from the same ice-core sections. Replicate ice-core analyses of measured [Fe_D] profiles with depth show a close correspondence in depth variation and a high degree of correlation. Determinations of [Fe_D] from the Antarctic Byrd ice-core, a low dust regime, yields a median of 0.033 $ng \cdot g^{-1}$ for preboreal ice, a median of 0.084 $ng \cdot g^{-1}$ for glacial ice, and a median of 0.131 $ng \cdot g^{-1}$ for LGM ice (Table S2). The Greenland ice-cores represent a much higher dust regime compared to the Antarctic ice-core sections, with a median of 0.134 $ng \cdot g^{-1}$ for Holocene ice and a median of 0.466 $ng \cdot g^{-1}$ for glacial ice.

For the described technique, we only quantify the biologically more important and easily leachable Fe fraction released in a controlled digestion step at pH ∼1.0. However, the degree of digestion varies with similar methods[28,29] using the same measurement principle and with methods using ICP-MS.[43] Therefore, a review and comparison of data from different operational methods for the determination Fe_D is difficult and further complicated by the limited determinations on temporally and spatially disparate ice-core samples. For example, the discrete digestion procedure and the elemental analyses of the combined insoluble and soluble fractions made with ICP-MS[43] yield [Fe_D] for Antarctic interglacial and glacial Talos Dome ice-core sections a magnitude greater than Fe_D determined by our methodology for preboreal, LGM, and glacial Byrd ice-core sections (Table S3, Supporting Information). In our measurements, determinations of Fe_D for Antarctic interglacial and glacial ice-core sections are below or closely approaching the 0.050 $ng \cdot g^{-1}$ LOD of earlier CFA methods.[28,29] For the case of Greenland ice the comparable DPD method by Spolaor et al.[28] shows preindustrial, late Holocene concentrations in the range of 0.05 (the LOD of their method) to 0.4 $ng \cdot g^{-1}$. Although their ice-core segment is much younger than our measurements on early to mid Holocene ice samples, it is interesting to note that the concentration ranges are identical. Moreover, we also see no significant concentration change within the three Holocene

time periods analyzed in our study (4.51, 6.55, and 7.61 kaBP). The very good agreement with the concentrations measured by Spolaor et al.[28] cannot be taken for granted, as they used a digestion step at pH 2, while we acidified to pH 1. Given the constant Fe levels in our three ice segments and the rather constant mineral dust-derived Ca^{2+} concentrations measured in Greenland over the entire Holocene,[44−46] we may assume also rather constant Fe concentrations. In this case the good correspondence of the values by Spolaor et al.[28] and our study suggests that a change in digestion pH from 2 to 1 does not influence the measurement results and that the release of the easily leachable fraction of Fe does require only modest acidification.

The solubility of aerosol metals in aqueous media (i.e., seawater, rainwater, cloudwater, and fresh water) are affected by a number of controlling factors, including solution pH,[47−51] crustal enrichment factor value of certain metals,[52,53] particle loading in solution,[53] aerosol type and size,[49,52,54,55] photoreduction,[56−58] and the presence of organic, acidic, or carbonaceous substances.[59−61] Accordingly, the amount of bioavailable Fe from aerosol deposition into the surface ocean is not only dependent on the pH of the surface ocean water bur largely controlled by the complex interplay of aerosol aging processes taking place in the atmosphere. Utilization of a specific aerosol metal solubility is further hindered by reference to a wide range of seawater solubility in previous studies, especially for Fe for studies by Hand et al.[62] and references therein. Evidence confirms that not all aeolian Fe, but only a dissolved fraction or specific speciation, is available for phytoplankton growth.[63,64] Recent studies have demonstrated that aeolian dissolvable Fe as well as Zn derived from long-range transport can stimulate marine production that is closely related to atmospheric CO_2 concentrations and thus also to climate change.[11,65−67] This relationship has also been confirmed by studies on marine sediment and ice-cores and by a series of in situ Fe-fertilizing experiments.[68−73] However, a more systematic investigation of the dependence of Fe digestion and the optimum pH to quantify bioavailable Fe is beyond the scope of this methodological paper and will be performed in the future.

The results demonstrate the successful adaptation of a colorimetric method for the determination of Fe_D concentrations in the low dust regime of the Antarctic Byrd ice-core and the high dust regime of the GRIP ice-core. The developed method employs a digestion step, which involves acidification of the aerosol dust in the ice-core sample. This mild digestion step involving a dilute Q-HCl decomposes Fe-hydroxides and Fe-complexes into dissolved free Fe, representing the easily leachable labile fraction and the working definition of the biological active fraction. This method will facilitate the quantification of acid leachable aerosol Fe flux to polar-regions via deposition and will eventually result in the improved assessment of the potential impacts of the biogeochemically active fraction of Fe on marine biogeochemistry in paleoclimatic studies.

The future usefulness of this and similar methods analyzing a fraction of Fe_T in a suspended dust sample hinge on the ability of the scientific community to arrive at a consensus for a methodological definition and singular description of the easily leachable labile Fe fraction, the analyte Fe_D, and the fraction representative of the biological available Fe. The degree of digestion could easily be modified and therefore allow for varied definitions of the easily leachable labile fraction of Fe_T in particulate dust particles in the ice-core to be analyzed. The primary factors controlling solubility of aerosol metals in digestion over a few minutes or less are solution pH, aerosol type, and aerosol size. Additional sample digestion experiments using standard reference material (i.e., AGV-1) are needed to determine if all but the most refractory metal species are being released into dissolved form. A single definition of Fe_D, representing the easily leachable labile fraction and the working definition of the biological active fraction, will allow the quantitative interlaboratory comparison of measurements. Dedicated studies of the bioavailable Fe and the pH dependence of its release during sample digestion have to be performed to validate the methodological definition of the easily leachable Fe fraction and the analyte Fe_D. The development of a standard/certified reference material (i.e., a dust suspension, AGV-1, in a low concentration buffer at a neutral pH representative of the matrix of ice-core meltwater) is a prerequisite to constructive interlaboratory comparison measurements.

Using our continuous CFA system, we were able to not only reliably quantify the mean Fe_D concentration for glacial high dust and interglacial low dust regimes both in Greenland and Antarctica but also to clearly resolve seasonal variations in Fe_D concentrations. These seasonal variations are on the order of a factor of 2−3 of the minimum seasonal values and are synchronous to the seasonality of other dust-derived aerosol tracers during all the studied climate periods. The resolution of our measurement could benefit from deconvolution of the measured signal, an algorithm-based process used to reverse the effects of dispersion, and memory effects by the CFA system in the recorded data. Further investigation of Fe_D, non-sea-salt Ca^{2+} ($nssCa^{2+}$), and dust correspondence in depth variation and degree of correlation may resolve and implicate nonuniformities depicted in Figure 1 and Figure S5 for the Antarctic Byrd ice-core during the LGM, further justifying the increased analytical effort for direct Fe_D determinations and providing detail not available with Fe deposition reconstructions calculated from the palaeoproxies dust and calcium.

■ ASSOCIATED CONTENT

Supporting Information

Details include a schematic of the CFA setup and the new Fe_D module and specifics regarding reagents, the Bern-CFA system, and the labile Fe detection method. Further information includes the following: results of the chemical parameter optimization measurement; calibration time-series, calibration curve, tabulated figures of merit; the results of test measurements of Antarctic Byrd ice-core and GRIP ice samples and tabulated data. This material is available free of charge via the Internet at http://pubs.acs.org.

■ AUTHOR INFORMATION

Corresponding Author

*Phone: +41(0) 31 631 8503. Fax: +41(0) 31 631 8742. E-mail: hiscock@climate.unibe.ch.

Notes

The authors declare no competing financial interest.

■ ACKNOWLEDGMENTS

We are grateful to Dr. René Nyffenegger for the utilization of the Perkin-Elmer LAMBDA 750 UV/vis/NIR spectrophotometer. Funding of W.T.H. was provided by the Double Career

Fund of the Rectors' Conference of the Swiss Universities (CRUS). Funding of the ice-core research has also been provided by the Swiss National Science Foundation (SNF).

REFERENCES

(1) Fischer, H.; Fundel, F.; Ruth, U.; Twarloh, B.; Wegner, A.; Udisti, R.; Becagli, S.; Castellano, E.; Morganti, A.; Severi, M.; Wolff, E.; Littot, G.; Röthlisberger, R.; Mulvaney, R.; Hutterli, M. A.; Kaufmann, P.; Federer, U.; Lambert, F.; Bigler, M.; Hansson, M.; Jonsell, U.; de Angelis, M.; Boutron, C.; Siggaard-Andersen, M.; Steffensen, J. P.; Barbante, C.; Gaspari, V.; Gabrielli, P.; Wagenbach, D. Reconstruction of millennial changes in dust emission, transport and regional sea ice coverage using the deep EPICA ice-cores from the Atlantic and Indian Ocean sector of Antarctica. *Earth Planet. Sci. Lett.* **2007**, *260*, 340−354.

(2) Wolff, E. W.; Fischer, H.; Fundel, F.; Ruth, U.; Twarloh, B.; Littot, G. C.; Mulvaney, R.; Röthlisberger, R.; de Angelis, M.; Boutron, C. F.; Hansson, M.; Jonsell, U.; Hutterli1, M. A.; Lambert, F.; Kaufmann, P.; Stauffer, B.; Stocker, T. F.; Steffensen, J. P.; Bigler, M.; Siggaard-Andersen, M. L.; Udisti, R.; Becagli, S.; Castellano, E.; Severi, M.; Wagenbach, D.; Barbante, C.; Gabrielli, P.; Gaspari, V. Southern Ocean sea-ice extent, productivity and iron flux over the past eight glacial cycles. *Nature* **2006**, *440*, 491−496.

(3) Lambert, F.; Bigler, M.; Steffensen, J. P.; Hutterli, M.; Fischer, H. Centennial mineral dust variability in high-resolution ice core data Dome C, Antarctica. *Clim. Past* **2012**, *8*, 609−623.

(4) Legrand, M.; Mayewski, P. A. Glaciochemistry of polar ice cores: A review. *Rev. Geophys.* **1997**, *35*, 219−143.

(5) Ahn, J.; Brook, E. J. Atmospheric CO_2 and climate on millennial time scales during the last glacial period. *Science* **2008**, *322*, 83−85.

(6) Bereiter, B.; Luthi, D.; Siegrist, M.; Schupbach, S.; Stocker, T. F.; Fischer, H. Mode change of millennial CO_2 variability during the last glacial cycle associated with a bipolar marine carbon seesaw. *Proc. Natl. Acad. Sci. U.S.A.* **2012**, *109* (25), 9755−9760.

(7) Röthlisberger, R.; Mulvaney, R.; Wolff, E. W.; Hutterli, M. A.; Bigler, M.; Sommer, S.; Jouzel, J. Dust and sea salt variability in central East Antarctica (Dome C) over the last 45 kyrs and its implications for southern high-latitude climate. *Geophys. Res. Lett.* **2002**, *29*, 2002GLO15186.

(8) Duce, R. A.; Liss, P. S.; Merrill, J. T.; Atlas, E. L.; Buat-Menard, P.; Hicks, B. B.; Millert, J. M.; Prospero, J. M.; Arimoto, R.; Church, T. M.; Ellis, W.; Galloway, J. N.; Hansen, L.; Jickells, T. D.; Knap, A. H.; Reinhardt, K. H.; Schneider, B.; Soudine, A.; Tokos, J. J.; Tsunogai, S.; Wollast, R.; Zhou, M. The atmospheric input of trace species to the world ocean. *Global Biogeochem. Cycles* **1991**, *5* (3), 193−259.

(9) Prospero, J. M.; Uematsu, M.; Savoie, D. L. Mineral aerosol transport to the Pacific Ocean. In *Chemical Oceanography*; Riley, J. P.; Chester, R., Eds.; Academic: London, 1989; Vol. *10*, pp 188−218.

(10) Johnson, K. S.; Gordon, R. M.; Coale, K. H. What controls dissolved iron concentrations in the world ocean? *Mar. Chem.* **1997**, *57*, 137−161.

(11) Martin, J. H.; Fitzwater, S. E. Iron deficiency limits phytoplankton growth in the north-east Pacific subarctic. *Nature* **1988**, *331*, 341−343.

(12) Greene, R. M.; Kolber, Z. S.; Swift, D. G.; Tindale, N. W.; Falkowski, P. G. Physiological limitation of phytoplankton photosynthesis in the eastern equatorial Pacific determined from variability in the quantum yield of fluorescence. *Limnol. Oceanogr.* **1994**, *39*, 1061−1074.

(13) Raven, J. A. Predictions of Mn and Fe use efficiencies of phototrophic growth as a function of light availability for growth and of C assimilation pathway. *New Phytol.* **1990**, *116*, 1−18.

(14) Chereskin, B. M.; Castelfranco, P. A. Effects of iron and oxygen on chlorophyll biosynthesis. *Plant Physiol.* **1982**, *68*, 112−116.

(15) Hiscock, W. T.; Millero, F. J. Nutrient and carbon parameters during the Southern Ocean iron experiment (SOFeX). *Deep-Sea Res., Part I* **2005**, *52*, 2086−2108.

(16) Menviel, L.; Joos, F.; Ritz, S. P. Simulating atmospheric CO_2, ^{13}C and the marine carbon cycle during the last glacial-interglacial cycle: possible role for a deepening of the mean remineralization depth and an increase in the oceanic nutrient inventory. *Quat. Sci. Rev.* **2012**, *56*, 46−68.

(17) Bock, M.; Schmitt, J.; Möller, L.; Spahni, R.; Blunier, T.; Fischer, H. Hydrogen isotopes preclude clathrate CH_4 emissions at the onset of Dansgaard-Oeschger events. *Science* **2010**, *328*, 1686−1689.

(18) Elsig, J.; Schmitt, J.; Leuenberger, D.; Schneider, R.; Eyer, M.; Leuenberger, M.; Joos, F.; Fischer, H.; Stocker, T. F. Stable isotope constraints on Holocene carbon cycle changes from an Antarctic ice core. *Nature* **2009**, *461*, 507−510.

(19) Schüpbach, S.; Federer, U.; Kaufmann, P. R.; Hutterli, M. A.; Buiron, D.; Blunier, T.; Fischer, H.; Stocker, T. F. A new method for high-resolution methane measurements on polar ice cores using continuous flow analysis. *Environ. Sci. Technol.* **2009**, *43*, 5371−5376.

(20) Stowasser, C.; Buizert, C.; Gkinis, V.; Chappellaz, J.; Schüpbach, S.; Bigler, M.; Faïn, X.; Sperlich, P.; Baumgartner, M.; Schilt, A.; Blunier, T. Continuous measurements of methane mixing ratios from ice cores. *Atmos. Meas. Tech.* **2012**, *5*, 999−1013.

(21) Bigler, M.; Röthlisberger, R.; Lambert, F.; Wolff, E. W.; Castellano, E.; Udisti, R.; Stocker, T. F.; Fischer, H. Atmospheric decadal variability from high-resolution Dome C ice core records of aerosol constituents beyond the Last Interglacial. *Quat. Sci. Rev.* **2010**, *29*, 324−337.

(22) Kaufmann, P.; Fundel, F.; Fischer, H.; Bigler, M.; Ruth, U.; Udisti, R.; Hansson, M.; de Angelis, M.; Barbante, C.; Wolff, E. W.; Hutterli, M.; Wagenbach, D. Ammonium and non-sea-salt sulfate in the EPICA ice cores as indicator of biological activity in the Southern Ocean. *Quat. Sci. Rev.* **2010**, *29*, 313−323.

(23) Ruth, U.; Barbante, C.; Bigler, M.; Delmonte, B.; Fischer, H.; Gabrielli, P.; Gaspari, V.; Kaufmann, P.; Lambert, F.; Maggi, V.; Marino, F.; Petit, J.; Udisti, R.; Wagenbach, D.; Wegner, A.; Wolff, E. W. Proxies and measurement techniques for mineral dust in Antarctic ice cores. *Environ. Sci. Technol.* **2008**, *42*, 5675−5681.

(24) McConnell, J. R.; Lamorey, G. W.; Lambert, S. W.; Taylor, K. C. Continuous ice-core chemical analyses using inductively coupled plasma mass spectrometry. *Environ. Sci. Technol.* **2002**, *36*, 7−11.

(25) Kuhn, H. R.; Günther, D. Laser ablation-ICP-MS: Particle size dependent elemental composition studies on filter-collected and online measured aerosols from glass. *J. Anal. At. Spectrom.* **2004**, *19*, 1158−1164.

(26) Thompson, M.; Coulter, J. E.; Sieper, F. Laser Aablation for the introduction of solid samples into an inductively coupled plasma for atomic emission spectrometry. *Analyst* **1981**, *106*, 32−39.

(27) Steffensen, J. P.; Andersen, K. K.; Bigler, M.; Clausen, H. B.; Dahl-Jensen, D.; Fischer, H.; Goto-Azuma, K.; Hansson, M.; Johnsen, S. J.; Jouzel, J.; Masson-Delmotte, V.; Popp, T.; Rasmussen, S. O.; Röthlisberger, R.; Ruth, U.; Stauffer, B.; Siggaard-Andersen, M. High-resolution Greenland ice core data show abrupt climate change happens in few years. *Science* **2008**, *321*, 680−684.

(28) Spolaor, A.; Vallelonga, P.; Gabrieli, J.; Roman, M.; Barbante, C. Continuous flow analysis method for the determination of soluble iron and aluminium in ice cores. *Anal. Bioanal. Chem.* **2013**, *405*, 767−774.

(29) Traversi, R.; Barbante, C.; Gaspari, V.; Fattori, I.; Largiuni, O.; Magaldi, L.; Udisti, R. Aluminium and iron record for the last 28 kyr derived from the Antarctic EDC96 ice core using new CFA methods. *Ann. Glaciol.* **2004**, *39*, 1−7.

(30) Johnson, K. S.; Boyle, E.; Bruland, K.; Measures, C.; Moffett, J. SAFe Team SAFe: Sampling and Analysis of Iron in the ocean. *Geophys. Res. Abstr.* **2005**, *7* (05813), 4−5.

(31) Measures, C. I.; Landing, W. M.; Brown, M. T.; Buck, C. S. A commercially available rosette system for trace metal−clean Sampling. *Limnol. Oceanogr.: Methods* **2008**, *6*, 384−394.

(32) Kaufmann, P. R.; Federer, U.; Hutterli, M. A.; Bigler, M.; Schüpbach, S.; Ruth, U.; Schmitt, J.; Stocker, T. F. An improved continuous flow analysis system for high-resolution field measurements on ice cores. *Environ. Sci. Technol.* **2008**, *42*, 8044−8050.

(33) Ruth, U.; Wagenbach, D.; Bigler, M.; Steffensen, J. P.; Röthlisberger, R.; Miller, H. High-resolution microplate profiles at

North GRIP, Greenland: Case studies of calcium-dust relationship. *Ann. Glaciol.* **2002**, *35*, 237−242.
(34) Hirayama, K.; Unohara, N. Spectrophotometric catalytic determination of an ultratrace amount of iron(III) in water based on the oxidation of *N,N*-dimethyl-*p*-phenylenediamine by hydrogen peroxide. *Anal. Chem.* **1988**, *60*, 2573−2577.
(35) Measures, C.; Yuan, J.; Resing, J. Determination of iron in seawater by flow injection analysis using in-line preconcentration and spectrophotometric detection. *Mar. Chem.* **1995**, *50*, 3−12.
(36) Weeks, D.; Bruland, K. Improved method for shipboard determination of iron in seawater by flow injection analysis. *Anal. Chim. Acta* **2002**, *453*, 21−32.
(37) Lunvongsa, S.; Tsubio, T.; Motomizu, S. Sequential determination of trace amounts of iron and copper in water samples by flow injection analysis with catalytic spectrophotometric detection. *Anal. Sci.* **2006**, *22*, 169−172.
(38) Moore, H.; Garmendla, M.; Cooper, W. Kinetics of monochloramine oxidation of *N,N*-diethyl-*p*-phenylenediamine. *Environ. Sci. Technol.* **1984**, *18*, 348−353.
(39) Ceriotti, G.; Spandrio, L. Spectrophotometric determination of ferric iron. *Anal. Chem.* **1961**, *33*, 579−580.
(40) Willie, S. N.; Iida, Y.; McLaren, J. W. Determination of Cu, Ni, Zn, Mn, Co, Pb, Cd, and V in seawater using flow injection ICP-MS. *Spectrochim. Acta, Part B* **1998**, *19*, 67−72.
(41) Hatta, M.; Measures, C. I.; Selph, K. E.; Zhou, M.; Yang, J. J.; Hiscock, W. T. Iron fluxes from the shelf regions near the South Shetland Islands in the Drake Passage during the austral-winter 2006. *Deep-Sea Res., Part II* **2013**.
(42) Milne, A.; Landing, W.; Bizimis, M.; Morton, P. Determination of Mn, Fe, Co, Ni, Cu, Zn, Cd and Pb in seawater using high-resolution magnetic sector inductively coupled mass spectrometry (HR-ICP-MS). *Anal. Chim. Acta* **2010**, *665*, 200−207.
(43) Spolaor, A.; Vallelonga, P.; Gabrieli, J.; Cozzi, G.; Boutronf, C.; Barbante, C. Determination of Fe^{2+} and Fe^{3+} species by FIA-CRC-ICP-MS in Antarctic ice samples. *J. Anal. At. Spectrom.* **2012**, *27*, 310−317.
(44) Mayewski, P. A.; Meeker, L. D.; Whitlow, S.; Twickler, M. S.; Morrison, M. C.; Grootes, P. M.; Bond, G. C.; Alley, R. B.; Meese, D. A.; Gow, A. J.; Taylor, K. C.; Ram, M.; Wumkes, M. Changes in atmospheric circulation and ocean ice cover over the North Atlantic during the last 41,000 years. *Science* **1994**, *263*, 1747−1751.
(45) Mayewski, P. A.; Meeker, L. D.; Twickler, M.; Whitlow, S.; Yang, Q.; Lyons, W. B.; Prentice, M. Major features and forcing of high-latitude northern hemisphere atmospheric circulation using a 110,000-year-long glaciochemical series. *J. Geophys Res.* **1997**, *102* (C12), 26345−26366.
(46) Fischer, H.; Siggaard-Andersen, M.-L.; Ruth, U.; Röthlisberger, R.; Wolff, E. Glacial/interglacial changes in mineral dust and sea salt records in polar ice cores: sources, transport, deposition. *Rev. Geophys.* **2007**, *45* (RG1002), doi: 10.1029/2005RG000192.
(47) Statham, P. J.; Chester, R. Dissolution of manganese from marine atmospheric particulates into seawater and rainwater. *Geochim. Cosmochim. Acta* **1988**, *52*, 2433−2437.
(48) Lim, B.; Jickells, T. D.; Colin, J. L.; Losno, R. Solubilities of Al, Pb, Cu and Zn in rain sampled in the marine environment over the North Atlantic Ocean and Mediterranean Sea. *Global Biogeochem. Cycles* **1994**, *8*, 349−362.
(49) Chester, R.; Nimmo, M.; Keyse, S.; Corcoran, P. A. Rainwater-aerosol trace metal relationships at Cape Ferrat: a coastal site in the Western Mediterranean. *Mar. Chem.* **1997**, *58*, 293−312.
(50) Chester, R.; Nimmo, M.; Fones, G. R.; Keyse, S.; Zhang, J. The solubility of Pb in coastal marine rainwaters: pH-dependent relationships. *Atmos. Environ.* **2000**, *34*, 3875−3887.
(51) Desboeufs, K. V.; Losno, R.; Vimeux, F.; Cholbi, S. The pH dependent dissolution of wind-transported Saharan dust. *J. Geophys. Res.* **1999**, *104*, 21287−21299.
(52) Chester, R.; Murphy, K. J. T.; Lin, F. J.; Berry, A. S.; Bradshaw, G. A.; Corcoran, P. A. Factors controlling the solubilities of trace metals from non-remote aerosols deposited to the sea surface by the 'dry' deposition mode. *Mar. Chem.* **1993**, *42*, 107−126.
(53) Guerzoni, S.; Molinaroli, E.; Rossini, P.; Rampazzo, G.; Quarantotto, G.; de Falco, G.; Cristini, S. Role of desert aerosol in metal fluxes in the Mediterranean Area. *Chemosphere* **1999**, *39*, 229−246.
(54) Davison, W.; Arewgoda, C. M.; Hamilton-Taylor, J.; Hewitt, C. N. Kinetics of Dissolution of Lead and Zinc from Rural Atmospheric Aerosols in Freshwater and Synthetic Solutions. *Water Res.* **1994**, *28*, 1703−1709.
(55) Chester, R.; Bradshaw, G. F.; Corcoran, P. A. Trace metal chemistry of the North Sea particulate aerosol; concentrations, sources and sea water fates. *Atmos. Environ.* **1994**, *28*, 2873−2883.
(56) Zhuang, G. S.; Yi, Z.; Duce, R. A.; Brown, P. R. Chemistry of iron in marine aerosols. *Global Biogeochem. Cycles* **1992**, *6*, 161−173.
(57) Zhu, X.; Prospero, J. M.; Millero, F. J.; Savioe, D. L.; Brass, G. W. The solubility of ferric ion in marine mineral aerosol solutions at ambient relative humidities. *Mar. Chem.* **1992**, *38*, 91−107.
(58) Zhu, X.; Prospero, J. M.; Savoie, D. L.; Millero, F. J.; Zika, R. G.; Saltzman, E. S. Photoreduction of iron(III) in marine mineral aerosol solutions. *J. Geophys. Res.* **1993**, *98*, 9039−9046.
(59) Zuo, Y. Kinetics of photochemical/chemical cycling of iron coupled with organic substances in cloud and fog droplets. *Geochim. Cosmochim. Acta* **1995**, *59*, 3123−3130.
(60) Desboeufs, K. V.; Losno, R.; Colin, J. L. Factors influencing aerosol solubility during cloud processes. *Atmos. Environ.* **2001**, *35*, 3529−3537.
(61) Desboeufs, K. V.; Sofikitis, A.; Losno, R.; Colin, J. L.; Ausset, P. Trace metals dissolution and solubility from mineral particles. *Chemosphere* **2005**, *58*, 195−203.
(62) Hand, J. L.; Mahowald, N. M.; Chen, Y.; Siefert, R. L.; Luo, C.; Subramaniam, A.; Fung, I. Estimates of atmospheric-processed soluble iron from observations and a global mineral aerosol model: Biogeochemical implications. *J. Geophys. Res.* **2004**, *109*, D17205.
(63) Hutchins, D.; Witter, A. E.; Butler, A.; Luther, G. W. Competition among marine phytoplankton for different chelated iron species. *Nature* **1999**, *400*, 858−861.
(64) Barbeau, K.; Moffett, J. Laboratory and field studies of colloidal iron oxide dissolution as mediated by phagotrophy and photolysis. *Limnol. Oceanogr.* **2000**, *45*, 827−835.
(65) Coale, K. H.; Johnson, K. S.; Fitzwater, S. E.; Gordon, R. M.; Tanner, S.; Chavez, F. P.; Ferioli, L.; Sakamoto, C.; Rogers, P.; Millero, F.; Steinberg, P.; Nightingale, P.; Cooper, D.; Cochlan, W. P.; Landry, M. R.; Constantinou, J.; Rollwagen, G.; Trasvinastar, A.; Kudela, R. A massive phytoplankton bloom induced by an ecosystem-scale iron fertilization experiment in the equatorial Pacific Ocean. *Nature* **1996**, *383*, 495−501.
(66) Cooper, D. J.; Watson, A. J.; Nightingale, P. D. Large decrease in ocean surface CO_2 fugacity in response to in situ iron fertilization. *Nature* **1996**, *383*, 511−513.
(67) Schulz, K. G.; Zondervan, I.; Gerringa, L. J. A.; Timmermans, K. R.; Veldhuis, M. J. W.; Riebesell, U. Effect of trace metal availability on coccolithophorid calcification. *Nature* **2004**, *430*, 673−676.
(68) Martin, J. H.; Coale, K. H.; Johnson, K. S.; Fitzwater, S. E.; Gordon, R. M.; Tanner, S. J.; Hunter, C. N.; Elrod, V. A.; Nowicki, J. L.; Coley, T. L.; Barber, R. T.; Lindley, S.; Watson, A. J.; Van Scoy, K.; Law, C. S.; Liddicoat, M. I.; Ling, R.; Stanton, T.; Stockel, J.; Collins, C.; Anderson, A.; Bidigare, R.; Ondrusek, M.; Latasa, M.; Millero, F. J.; Lee, K.; Yao, W.; Zhang, J. Z.; Friederich, G.; Sakamoto, C.; Chavez, F.; Buck, K.; Kolber, Z.; Greene, R.; Falkowski, P.; Chisholm, S. W.; Hoge, F.; Swift, R.; Yungel, J.; Turner, S.; Nightingale, P.; Hatton, A.; Liss, P.; Tindale, N. W. Testing the iron hypothesis in ecosystems of the equatorial Pacific. *Nature* **1994**, *371*, 123−129.
(69) Kumar, N.; Anderson, R. F.; Mortlock, R. A.; Froelich, P. N.; Kubik, P.; Dittrichhannen, B.; Suter, M. Increased biological productivity and export production in the glacial Southern-Ocean. *Nature* **1995**, *378*, 675−680.
(70) Petit, J. R.; Jouzel, J.; Raynaud, D.; Barkov, N. I.; Barnola, J.; Basile, I.; Bender, M.; Chappellaz, J.; Davisk, M.; Delaygue, G.;

Delmotte, M.; Kotlyakov, V. M.; Legrand, M.; Lipenkov, V. Y.; Lorius, C.; Pépin, L.; Ritz, C.; Saltzmank, E.; Stievenard, M. Climate and atmospheric history of the past 420,000 years from the Vostok core, Antarctica. *Nature* **1999**, *399*, 429−436.

(71) Boyd, P. W.; Watson, A. J.; Law, C. S.; Abraham, E. R.; Trull, T.; Murdoch, R.; Bakker, D. C. E.; Bowie, A. R.; Buesseler, K. O.; Chang, H.; Charette, M.; Croot, P.; Downing, K.; Frew, R.; Gall, M.; Hadfield, M.; Hall, J.; Harvey, M.; Jameson, G.; LaRoche, J.; Liddicoat, M.; Ling, R.; Maldonado, M. T.; McKay, R. M.; Nodder, S.; Pickmere, S.; Pridmore, R.; Rintoul, S.; Safi, K.; Sutton, P.; Strzepek, R.; Tanneberger, K.; Turner, S.; Waite, A. Zeldis, A mesoscale phytoplankton bloom in the polar Southern Ocean stimulated by iron fertilization. *Nature* **2000**, *407*, 695−702.

(72) Bopp, L.; Kohfeld, K. E.; Le Quere, C.; Aumont, O. Dust impact on marine biota and atmospheric CO_2 during glacial periods. *Paleoceanography* **2003**, *18*, 1046.

(73) Coale, K. H.; Johnson, K. S.; Chavez, F. P.; Buesseler, K. O.; Barber, R. T.; Brzezinski, M. A.; Cochlan, W. P.; Millero, F. J.; Falkowski, P. G.; Bauer, J. E.; Wanninkhof, R. H.; Kudela, R. M.; Altabet, M. A.; Hales, B. E.; Takahashi, T.; Landry, M. R.; Bidigare, R. R.; Wang, X. J.; Chase, Z.; Strutton, P. G.; Friederich, G. E.; Gorbunov, M. Y.; Lance, V. P.; Hilting, A. K.; Hiscock, M. R.; Demarest, M.; Hiscock, W. T.; Sullivan, K. F.; Tanner, S. J.; Gordon, R. M.; Hunter, C. N.; Elrod, V. A.; Fitzwater, S. E.; Jones, J. L.; Tozzi, S.; Koblizek, M.; Roberts, A. E.; Herndon, J.; Brewster, J.; Ladizinsky, N.; Smith, G.; Cooper, D.; Timothy, D.; Brown, S. L.; Selph, K. E.; Sheridan, C. C.; Twining, B. S.; Johnson, Z. I. Southern ocean iron enrichment experiment: Carbon cycling in high and low Si waters. *Science* **2004**, *304*, 408−414.